Oxyhalogen−Sulfur Chemistry: Kinetics and Mechanism of Oxidation of Guanylthiourea by Acidified Bromate[1]

Edward Chikwana, Adenike Otoikhian, and Reuben H. Simoyi*

Department of Chemistry, Portland State University, Portland, Oregon 97207-0751

Received: September 10, 2004; In Final Form: October 15, 2004

This article reports on the kinetics and mechanism of oxidation of the biologically active molecule guanylthiourea (GTU) by acidic bromate. This was a follow-up of a previous study in which mild oxidizing agents acidic iodate and molecular iodine oxidized GTU to a ring-cyclized product: 3,5-diamino-1,2,4-thiadiazole. In contrast, acidic bromate and molecular bromine, as stronger oxidizing agents, were able to oxidize GTU all the way to a complete desulfurization to yield guanylurea. No N-bromination was observed on any of the amino groups on guanylurea. The stoichiometry of the reaction was deduced to be $4BrO_3^- + 3H_2N(=NH)CNH(C=S)NH_2 + 3H_2O \rightarrow 4Br^- + 3H_2N(=NH)CNH(C=O)NH_2 + 3SO_4^{2-} + 6H^+$. In excess bromate conditions in which the ratio of oxidant to reductant $R = [BrO_3^-]_0/[GTU]_0 > 1.6$, the stoichiometry of the reaction was $8BrO_3^- + 5H_2N(=NH)CNH(C=S)NH_2 + H_2O \rightarrow 4Br_2(aq) + 5H_2N(=NH)CNH(C=O)NH_2 + 5SO_4^{2-} + 2H^+$. The direct reaction of aqueous bromine with GTU was extremely fast with an estimated lower limit bimolecular rate constant of $7.5 \pm 1.2 \times 10^4\ M^{-1}\ s^{-1}$. This rapid reaction with bromine produced reaction dynamics which involved bromine formation after a short induction period which was determined by the time it took for the complete oxidation of GTU and its oxidation intermediates. The mechanism of the reaction involved the initial formation of the ring-cyclized 3,5-diamino-1,2,4-thiadiazole which was later successively oxidized through the sulfoxide and sulfone, followed by the opening of the ring to yield sulfate and guanylurea. All the observed global reaction dynamics were satisfactorily modeled by a simple mechanism involving 14 elementary reactions.

Introduction

Guanylthiourea, GTU, is an important biological and industrial molecule. Its special structure enables it to be used in the synthesis of anion-caged supermolecular compounds,[2] and it is also one of the most important accelerators in vulcanization of natural rubber.[3−7] In medicine, it is used as a stimulator of intestinal peristalsis[8] and *S*-allyl-guanylthiourea has been investigated as a possible immunostimulant and tumor cell inhibitor.[9,10]

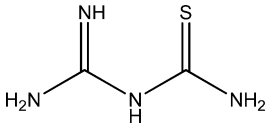

guanylthiourea

The general conjecture is that physiological effects of bioactive thiocarbamides, such as GTU, are effected by their metabolites rather than the intact molecules themselves.[11] The only possible metabolites of thiocarbamides are the thiyl radicals, possible dimers, and the series of oxoacids that are formed upon oxidation of the sulfur center.[12] Our laboratory recently embarked on a series of studies aimed at unraveling S-oxygenation mechanisms and possible metabolites of several bioactive organosulfur compounds.[13] The oxidation of GTU by acidic iodate was recently studied in our laboratories.[14] The reaction dynamics surprisingly delivered exotic behavior that was characterized by clock reaction characteristics and oligooscillatory formation of iodine in conditions of both excess oxidant and excess reductant. The oxidation product was a ring-cyclized product of GTU after a two-electron oxidation: 3,5-diamino-1,2,4-thiadiazole. There was no further oxidation past this product. The global dynamics of the reaction appeared to be iodide-controlled, with iodide playing a pivotal role in the induction periods observed from clock reaction behavior, amount of transient iodine formed, as well as rate of consumption of iodine at the end of the reaction in excess reductant conditions. Previous studies of the oxidation of GTU by the biological oxidant H_2O_2 had also shown a wide range of products with the ring-cyclized product dominating.

We report in this article on the oxidation mechanism of GTU by acidic bromate. The use of bromate, which is a stronger oxidizing agent than iodate, was to determine if the oxidation of GTU could go past the ring-cyclized product, and what other oxidation products are possible. Of interest was whether the sulfinic and sulfonic acids could be isolated and further studied. It is still our assertion that the C−S bond is easier to cleave at the sulfinic and sulfonic acid stages of oxidation of a thiocarbamide[15] and that this cleavage brings with it inadvertent toxicity by the formation of reactive oxygen species.[16−18]

Experimental Section

Reagents. Distilled deionized water was used for preparation of all stock solutions (Barnstead Sybron Corp. water purification unit). Inductively-coupled plasma mass spectrometry, ICPMS, was used to evaluate concentrations of metal ions in the reagent water. ICPMS results showed negligible amounts (>0.1 ppb) of copper, iron, and silver ions with approximately 1.5 ppb of cadmium and 0.43 ppb of lead as the highest metal ion concentrations. No discernible differences in kinetics data were obtained between experiments run with chelators (EDTA, deferroxamine) and those run without, and so all experiments

10.1021/jp045897r CCC: $27.50
Published on Web 12/04/2004

were carried out without the use of chelators. The following reagents were used without further purification: guanylthiourea, 97% (Acros), sodium bromate (Aldrich), sodium bromide, sodium perchlorate, and perchloric acid (70%) (Fisher). Standard bromine solutions were prepared by diluting liquid bromine under a strong fume hood and standardizing it by adding excess iodide which was then titrated against sodium thiosulfate with starch indicator. This standardization was utilized to evaluate an absorptivity coefficient of 142 M^{-1} cm^{-1} for aqueous bromine at 390 nm. Bromine solutions were standardized every day before use. Stock solutions of GTU were also prepared fresh daily and protected from light by covering with aluminum foil and storing in the dark.

Methods. Reactions were run at a constant ionic strength of 1.0 M by adding the required amount of sodium perchlorate. The reaction temperature was maintained at 25 ± 0.5 °C using a Neslab RTE 101 thermostat bath. The kinetics of the two reaction systems studied, BrO_3^-−GTU and Br_2−GTU, were followed on a Hi-Tech Scientific Double-Mixing SF61-DX2 stopped-flow spectrophotometer. Digitization and amplifying were done via an Omega Engineering DAS-50/1 16-bit A/D board interfaced to a Pentium IV computer. Sodium bromate, perchloric acid, and sodium perchlorate were premixed in one vessel at double the reactor concentrations as one of the reagent solutions, with the other solution containing only GTU.

Stoichiometric Determinations. Stoichiometric determination of the bromate−GTU reaction was performed both in excess BrO_3^- and in excess GTU. In the former case, the total oxidizing power of the product solution (BrO_3^- + Br_2) was determined by titration. Excess acidified iodide was added to the reaction solution, and the released iodine was titrated against standard thiosulfate. Sulfate was qualitatively tested and quantitatively determined as a barium sulfate precipitate. Bromine formed in excess BrO_3^- was also determined separately by its absorbance at 390 nm (ϵ = 142 M^{-1} cm^{-1}). The stoichiometry of the direct Br_2−GTU reaction was determined spectrophotometrically and by titration. Standardized bromine solution was titrated from a buret into a GTU solution of known strength. The end point of the titration could be detected as the point where the bromine color lingers. This end point could also be enhanced by starch indicator spiked with micromolar concentrations of iodide ions from the preservative HgI_2.[19]

Results

Reaction Dynamics. The bromate−GTU reaction represents a typical clock reaction in which initially there is a quiescent period in which the reaction shows no activity in the primary indicators of redox potential and absorbance changes at 390 nm. After an induction period whose length is determined by the initial reagent conditions, there is a sudden formation of aqueous bromine and a rapid increase in the redox potential which is dominated by the 1.08 V of the bromine/bromide couple. GTU has an isolated absorbance peak at 266 nm (absorptivity coefficient, 1.13 × 10^4 M^{-1} cm^{-1}), and if the reaction is monitored at this wavelength, an initially slow sigmoidal decay in the absorbance reading is observed, even during the induction period when there is no activity at 390 nm. Clock behavior only occurs when bromate concentrations are in large stoichiometric excess over GTU.

Stoichiometry and Product Determination. The observed clock behavior does suggest the possibility of more than one stoichiometry. Several reaction solutions with varying ratios of bromate to GTU were prepared and allowed to sit for periods of up to 24 h. They were then analyzed spectrophotometrically, at 390 nm, for the presence of bromine. Figure 1a shows six such experiments. The only solutions which showed bromine formation were those in which the oxidant to reductant ratio, $R = [BrO_3^-]_0/[GTU]_0$, was greater than 1.333. Larger ratios gave higher final bromine concentrations until they reached a maximum at approximately R = 1.60. These solutions were also further analyzed for excess oxidizing power: ($[BrO_3^-]_\infty$ + $[Br_2]_\infty$) by the standard iodometric techniques, and a plot of thiosulfate volume required vs initial bromate concentrations was created (Figure 1b). The idea behind such a plot was to quantify the amount of bromate left after reaction with a fixed amount of GTU. This would aid in evaluating the stoichiometry of the reaction just before the formation of bromine. The conjecture is that formation of bromine would result from the reaction of excess bromate with the bromide product obtained from the reduction of bromate. Thus, in the absence of a stoichiometric excess of bromate, the reaction would not "clock". If the reaction of bromine with GTU is fast, then this clocking would be very sharp and can be used as an indicator for complete consumption of GTU. The exact molarity and

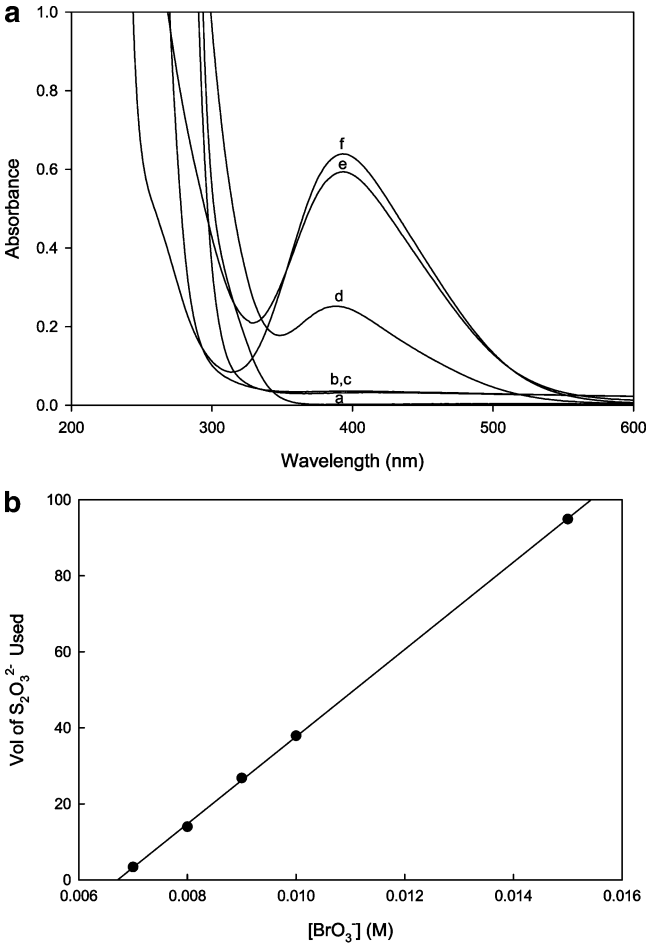

Figure 1. (a) Spectral scan for stoichiometric analysis (of product solutions) showing the accumulation of bromine at 390 nm in the bromate oxidation of GTU. In stoichiometric excess of GTU (a−c), there is no bromine formation, but for $R = [BrO_3^-]_0/[GTU]_0 > 1.333$ (d−f) bromine is formed as one of the final products. $[GTU]_0$ = 0.005 M; $[H^+]_0$ = 0.25 M; $[BrO_3^-]_0$ = (a) 0.001, (b) 0.004, (c) 0.005, (d) 0.007, (e) 0.008, (f) 0.015 M. (b) Titration results for the experiments shown in panel a. For a constant GTU concentration of 0.005 M, the intercept on the $[BrO_3^-]$ axis is 0.00667 M. This intercept represents the maximum amount of bromate tolerated by the reaction system before permanent bromine production is observed. This will fall on stoichiometry R1 which gives a ratio of 4/3.

strength of the thiosulfate solution used in the data shown in Figure 1b are not important. What is important are the moles of bromate (for fixed GTU concentrations) that will deliver zero titer in thiosulfate (obtained by extrapolation to the bromate concentration axis). This will give the exact number of moles of bromate needed to just completely oxidize GTU with no bromate left over to form bromine with the bromide product. In the plot shown in Figure 1b, the strength of the GTU solution used was constant in all experiments as 0.005 M. Titration results show that no excess oxidizing power is available when $[BrO_3^-]_0 = 0.00667$ M (intercept on the bromate concentration axis). This simplifies to a 4:3 ratio with a stoichiometric reaction of

$$4BrO_3^- + 3H_2N(=NH)CNH(C=S)NH_2 + 3H_2O \rightarrow 4Br^- + 3H_2N(=NH)CNH(C=O)NH_2 + 3SO_4^{2-} + 6H^+ \quad (R1)$$

with the major oxidation product being guanylurea. Reagent grade guanylurea (sulfate salt) gave a UV spectrum that was identical to the one obtained from the product solution in stoichiometry R1. Proton NMR and carbon-13 spectra of the product solution (in DCl) were identical to those obtained from literature for guanylurea. Gravimetric analysis of sulfate as $BaSO_4$ gave a 1:1 ratio of GTU to sulfate formed within 95% of that expected from R1. Qualitative tests for ammonium ions, which are possible hydrolysis products of guanylurea, were negative. In excess bromate conditions, the bromide product in stoichiometry R1 reacted with bromate to produce aqueous bromine:[20]

$$BrO_3^- + 5Br^- + 6H^+ \rightarrow 3Br_2(aq) + 3H_2O \quad (R2)$$

The overall reaction stoichiometry in excess bromate was thus a linear combination of stoichiometries R1 and R2 to eliminate bromide; 5R1 + 4R2:

$$8BrO_3^- + 5H_2N(=NH)CNH(C=S)NH_2 + H_2O \rightarrow 4Br_2(aq) + 5H_2N(=NH)CNH(C=O)NH_2 + 5SO_4^{2-} + 2H^+ \quad (R3)$$

A complementary test for stoichiometry R3 was the absorbance of aqueous bromine at 390 nm. In high excess of bromate, $[BrO_3^-]_0/[GTU]_0 > 10$, the amount of bromine obtained was proportional to the initial concentrations of GTU (see Figures 2a, 3a, and 4a). Experimental data showed that the amount of aqueous bromine produced was approximately 80% in moles compared to initial GTU concentrations, which is the stoichiometry reflected in R3. Titrimetric and spectrophotometric techniques established that the stoichiometry of the direct Br_2−GTU reaction was 4:1:

$$4Br_2(aq) + H_2N(=NH)CNH(C=S)NH_2 + 5H_2O \rightarrow 8Br^- + SO_4^{2-} + H_2N(=NH)CNH(C=O)NH_2 + 10H^+ \quad (R4)$$

Kinetics Data. The reaction displayed all the normal characteristics of an organosulfur−oxybromine reaction with a delayed production of bromine after an induction period.[21] Figure 2a shows a series of experiments carried out with varying initial bromate concentrations while keeping all other parameters invariant. The data show that in high excess of bromate, the amount of bromine formed is invariant (see stoichiometry R3),

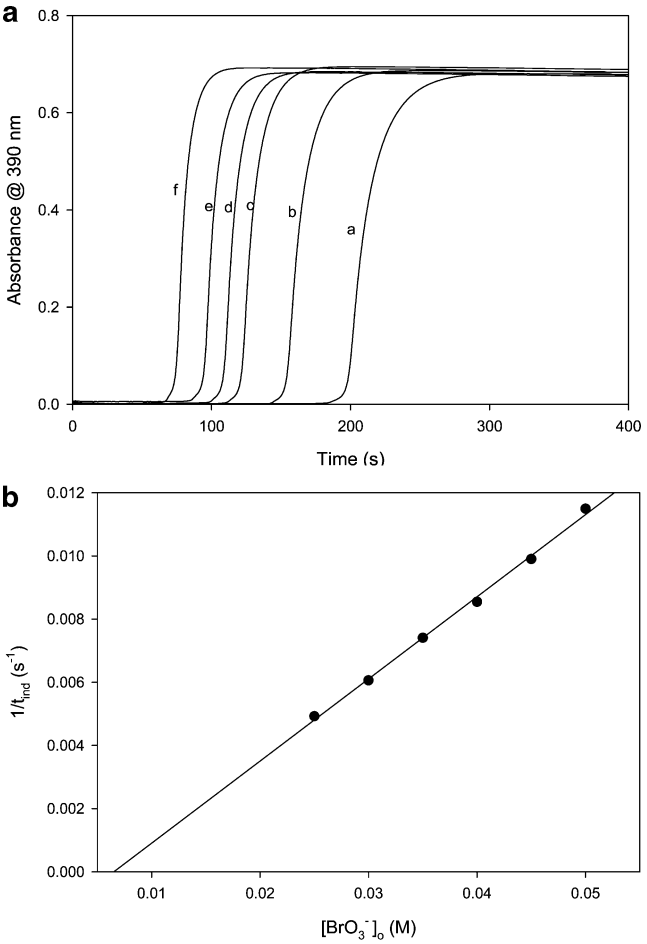

Figure 2. (a) Effect of $[BrO_3^-]$ variation at constant $[H^+]_0$ and $[GTU]_0$ showing a finite and measurable induction period before formation of bromine. For as long as $R > 1.600$, the final moles of bromine formed is invariant with changes in bromate and acid. $[GTU]_0 = 0.005$ M; $[H^+]_0 = 0.5$ M; $[BrO_3^-]_0 =$ (a) 0.025, (b) 0.030, (c) 0.035, (d) 0.040, (e) 0.045, (f) 0.050 M. (b) Linear plot of reciprocal induction time vs $[BrO_3^-]_0$ for data shown in panel a. The amount of initial bromate concentration indicated by the $[BrO_3^-]_0$ axis intercept is also equivalent to stoichiometry R1.

and that the period taken before formation of bromine is inversely proportional to the initial bromate concentrations to the first power. This is shown in Figure 2b where the intercept observed on the $[BrO_3^-]_0$ axis of 0.0066 M gives the exact amount of bromate needed to attain stoichiometry R1 without formation of bromine from excess bromate. Since the initial GTU concentrations used for data shown in Figure 2b were fixed at 0.005 M, this plot also confirms the 4:3 stoichiometry. Figure 3a shows data collected at varying acid concentrations. The induction period is now inversely proportional to the square of the acid concentrations as a plot of induction period vs inverse acid concentration squared gives a straight line (Figure 3b). Linearity in this plot is maintained for a wide range of acid concentrations with a saturation attained only at very high acid concentrations which we could not attain in this study due to the ionic strength requirements set for the whole study. The reaction reacted differently to GTU concentrations depending upon the ratio of oxidant to reductant. Figure 4a shows that in high excess of bromate, the induction period does not change with variations in GTU concentrations;[22] what changes is the rate and amount of bromine formed according to stoichiometry R3. At low oxidant to reductant ratios, $1.333 < R < 4.00$, the induction period lengthens with increasing $[GTU]_0$ (see Figure

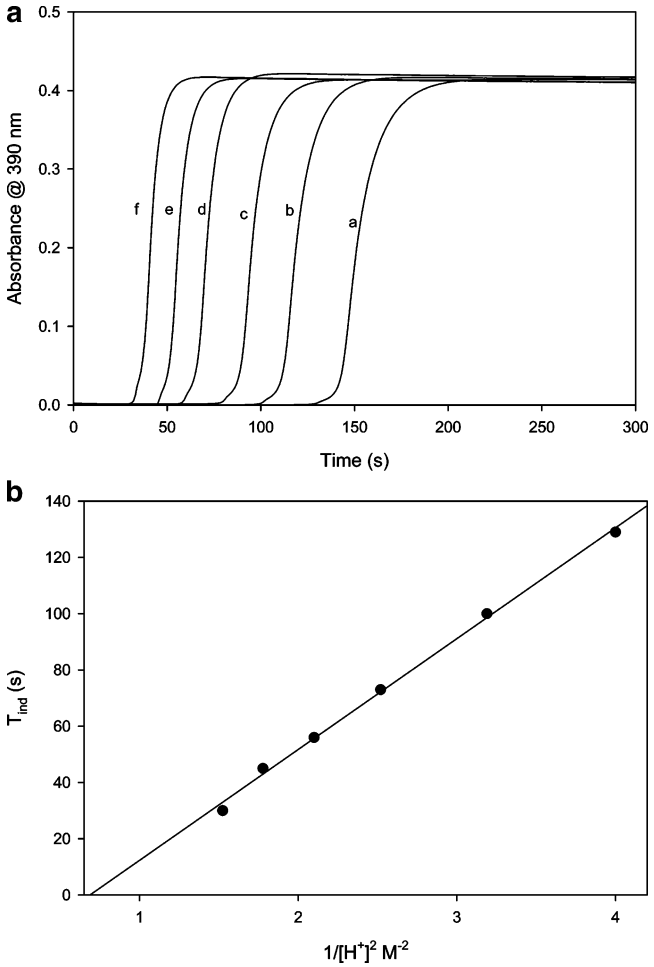

Figure 3. (a) For reactions run in excess bromate, an increase in $[H^+]$ strongly catalyzes the reaction by reducing the induction period and increasing the rate of formation of bromine at the end of this induction period at $R = 10$. $[GTU]_0 = 0.003$ M; $[BrO_3^-]_0 = 0.03$ M; $[H^+]_0 =$ (a) 0.50, (b) 0.56, (c) 0.63, (d) 0.69, (e) 0.75, (f) 0.81 M. Two of these traces (a,e) were simulated, and the results are shown in Figure 9. (a) Plot showing the linear dependence of induction time on the reciprocal of $[H^+]^2$ for data shown in panel a. This strong squared dependency on acid suggests domination of the standard oxybromine kinetics.

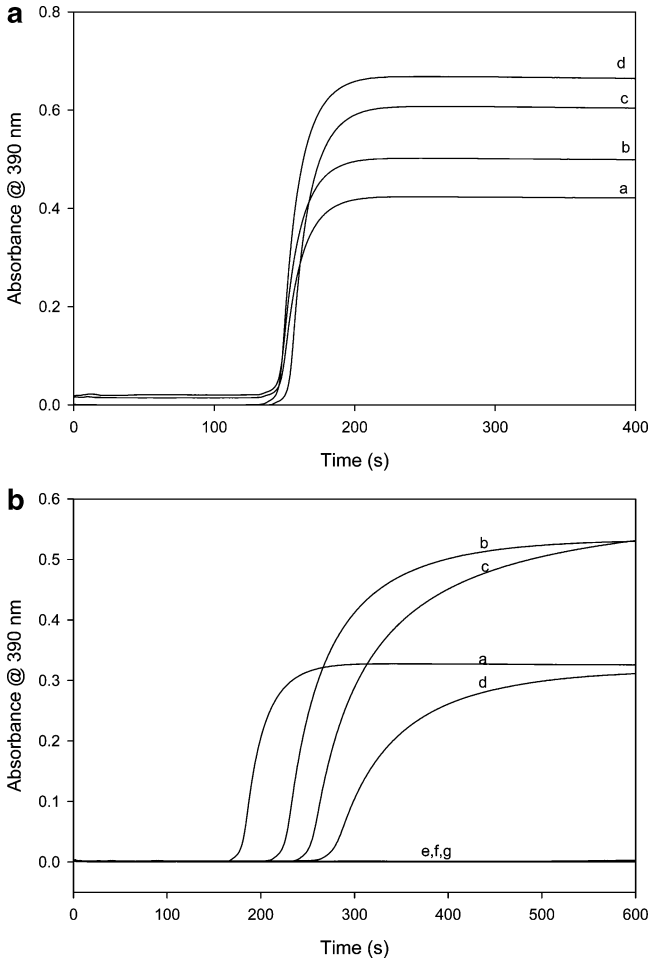

Figure 4. (a) GTU variation in excess oxidant shows no change in induction period. Higher GTU concentrations give higher rates of bromine production as well as higher final concentrations of bromine at the end of the reaction. In all the traces shown in this figure, $R >$ 1.6 and hence the variation of bromine concentrations formed with GTU. $[BrO_3^-]_0 = 0.03$ M; $[H^+]_0 = 0.5$ M; $[GTU]_0 =$ (a) 0.003, (b) 0.0035, (c) 0.0045, (d) 0.005 M. (b) Traces showing the effect of varying GTU close to the stoichiometric point. Initially the absorbance increases (traces a and b), but as R approaches 1.333 (trace e) it starts to decrease. For $R < 1.333$ (traces f and g), no bromine is produced. $[BrO_3^-]_0 = 0.007$ M; $[H^+]_0 = 0.875$ M; $[GTU]_0 =$ (a) 0.0025, (b) 0.0040, (c) 0.0045, (d) 0.0050, (e) 0.00525, (f) 0.006, (g) 0.007 M.

4b). As the induction period lengthens, the amount of bromine formed also increases until $R = 1.600$ at which point further increases in $[GTU]_0$ will not show any further increase in amount of bromine formed (stoichiometry R3).

Data Collected at 266 nm. We utilized the sharp isolated absorbance peak of GTU at 266 nm to follow the initial rate of consumption of GTU. Guanylurea and an as-yet-unidentified intermediate also absorb at this peak, and thus, for kinetics data collection only the initial 5% of the reaction was considered. Figure 5a shows traces at 266 nm with an initial decay in the absorbance followed by a transient increase due to the accumulation of an intermediate and then a monotonic decay to form guanylurea and sulfate. An evaluation of dependence of initial rates with acid concentrations gave neither first-order nor second-order dependence at these high acid concentrations but clearly gave second-order kinetics with respect to acid concentrations for lower acid concentrations ranging from 0.30 to 0.60 M. Initial rates, however, were found to be directly proportional to bromate concentrations for all ranges of bromate concentrations studied. Figure 5b superimposes two sets of absorbance traces at the same initial concentrations, with one at 266 nm (GTU depletion) and the other at 390 nm (bromine formation). These data show that the reactions of bromine with GTU and all its possible intermediates are so rapid that no bromine formation occurs until they are all consumed since the end of the induction period coincides with the end of absorbance activity at 266 nm. This, however, makes the identification of the transient intermediate shown in Figure 5a more difficult.

Nature of the Intermediate Species at 266 nm. Traces of the type shown in Figure 5a were studied by the rapid-scan technique. Figure 6a shows a series of spectral scans taken every minute up to the point where the decrease in absorbance at 266 nm stops and the transient increase in absorbance is observed. This spectrum also shows a monotonic increase in the peak at 248 nm. A continuation of these spectral scans shown in Figure 6b indicates that the observed increase in absorbance is due to a species that has an absorption peak at 260 nm but also has a reasonably high absorbance at the absorption wavelength of 266 nm. This peak later decays to give the UV spectrum of the product guanylurea. While the tribromide species does absorb considerably at 260 nm, the overall observed UV/vis spectrum did not match with that of a mixture of aqueous bromine in 1.0 M NaBr. Data in Figure 5b also show that no tribromide species should exist during the formation of this intermediate since

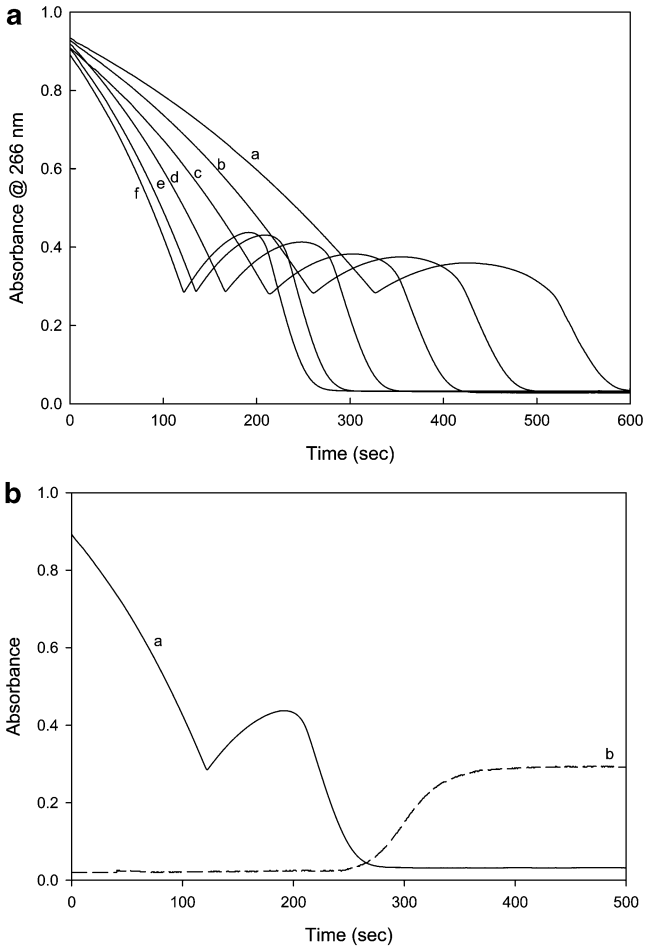

Figure 5. (a) Absorbance traces showing the effect of increasing acid concentration on the consumption of guanylthiourea. $[BrO_3^-]_0 = 0.007$ M; $[GTU]_0 = 1.0 \times 10^{-4}$ M; $[H^+]_0 =$ (a) 0.5, (b) 0.55, (c) 0.65, (d) 0.70, (e) 0.75 M. The transient peaks observed are derived from the equilibrium between the folded and straight-chain guanylthiourea sulfur oxo-acid intermediates. (b) Traces showing the superimposition of absorbance traces taken at 266 nm (a, solid line) and at 390 nm (b, dashed line). The trace followed in experiment f in panel a. This figure shows that the transient intermediate formed is not from Br_3^- since formation of bromine only commences after this transient intermediate is completely consumed.

bromine formation only commences after the total consumption of GTU and its oxidation intermediates. The intermediate species formed, then, can be deduced to arise from the transformation between the cyclized and open-chain versions of guanylthiourea oxidation metabolite sulfone (step d in pathway B). To prove this fact, two further sets of experiments were performed. The first one involved the use of the rapid-scan technique for the oxidation of GTU by iodate for which mass spectrometry had already established the cyclized 3,5-diamino-1,2,4-thiadiazole as the major product. The final UV/vis spectrum observed was identical to that observed for the intermediate species (Figure 6a,b). The second set of experiments involved the reaction of GTU with carefully measured equivalents of aqueous bromine. The series of the final spectra obtained is shown in Figure 6c. This set of experiments shows that although GTU has a peak at 266 nm, as soon as the reaction commences, this peak shifts to 260 nm. This peak is gradually decreased by addition of more equivalents of bromine until at the stoichiometric point of 4 equiv to 1 equiv of GTU, this peak vanishes to give way to the spectrum of guanylurea. The transient formation of this peak is

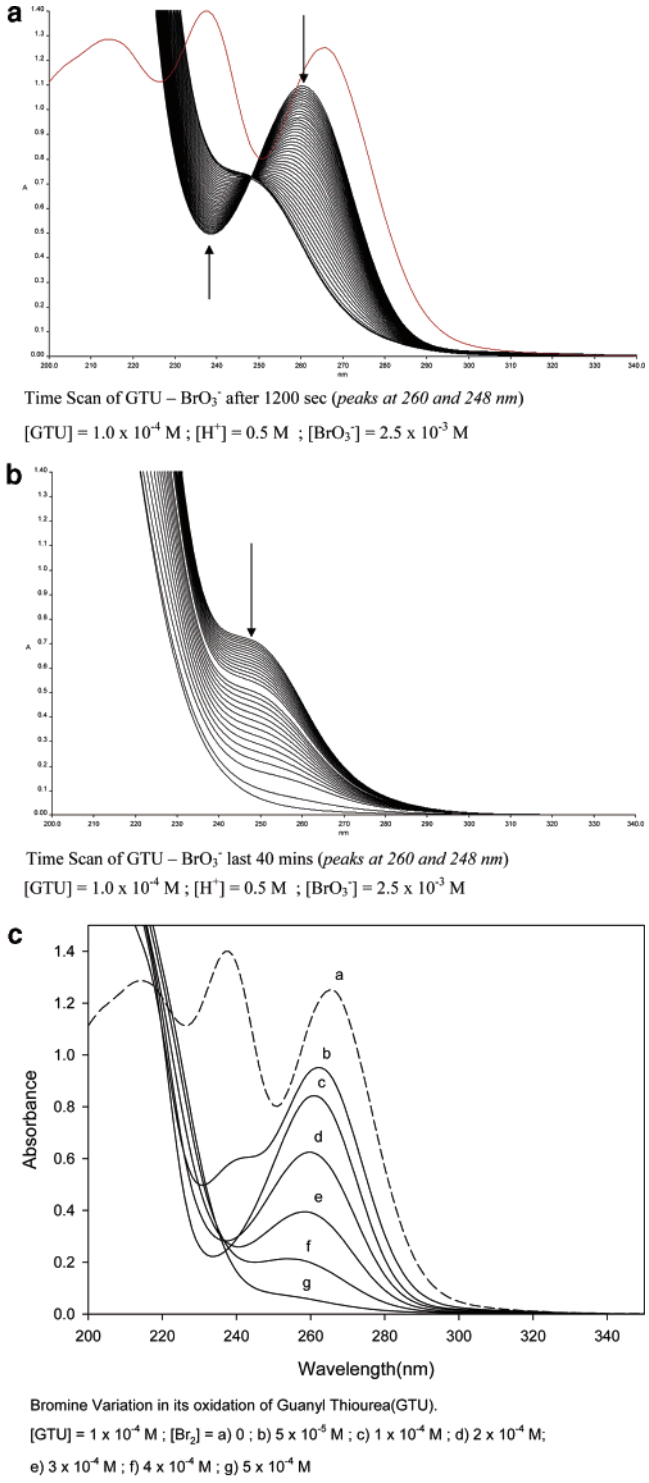

Figure 6. (a) Rapid-scan spectra taken every 5 s of a typical trace shown in Figure 5a. This figure shows the appearance of the spectra up to the point where the absorbance at 266 nm starts to increase (this could be equivalent to the first 100 s of trace f in Figure 5a. Notice that as soon as the reaction commences the absorption peak changes from 266 to 260 nm. (b) The latter stages of the same trace shown in panel a. In this figure there is a monotonic decrease in the peak at 260 nm. This transient spectrum that decays is identical to that obtained for the product of the iodate−TU reaction which was confirmed to the ring-cyclized 3,5-diamino-1,2,4-thiadiazole. (c) Final spectra obtained with different bromine equivalents to 1 equiv of GTU. This shows the absence of any new species nor the existence of an oxo-acid intermediate that absorbs radically differently from the others to justify the transient peak observed in Figure 5a. The different bromine equivalents consume, spectrophotometrically, the correct amounts of GTU based on stoichiometry R4.

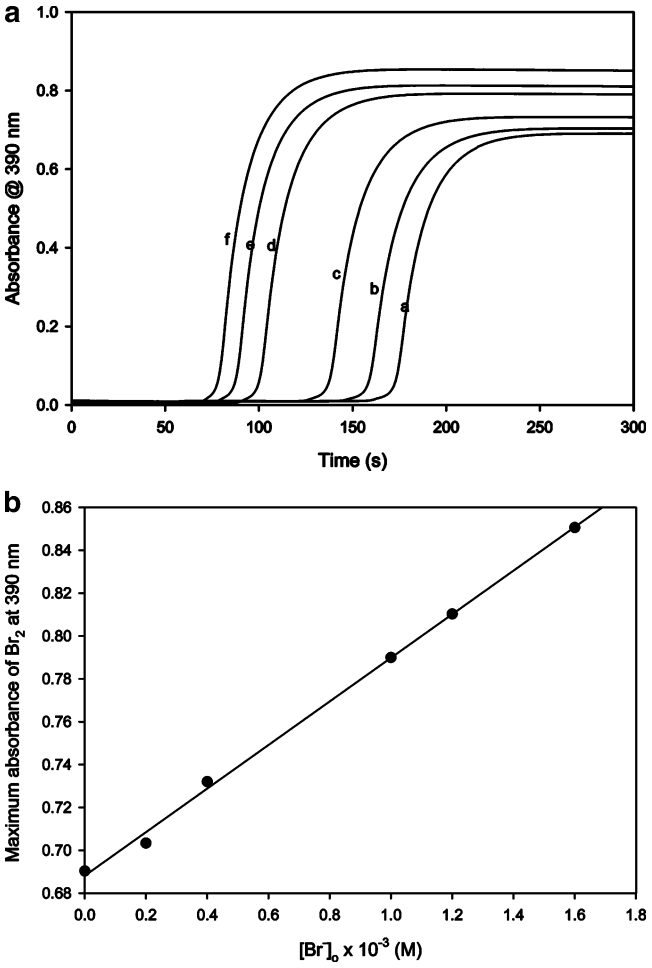

Figure 7. (a) Bromide effect on the GTU−bromate reaction. The effect of bromide can be seen on the reduced induction period and increased final bromine concentration as initial bromide ions are increased. $[GTU]_0 = 0.005$ M; $[H^+]_0 = 0.5$ M; $[BrO_3^-]_0 = 0.03$ M; $[Br^-]_0 =$ (a) 0, (b) 0.0002, (c) 0.0004, (d) 0.0010, (e) 0.0012, (f) 0.0016 M. (b) Plot showing linear increase in maximum bromine concentrations as for data shown in panel a. Maximum absorbances are as expected from a combination of stoichiometries R2 + R3. This proves the absence of the formation of *N*-bromamines on the amino groups of GTU and guanylurea.

not observed in this series of experiments because the spectra shown are after a 24-h incubation period after all transients have ebbed and equilibriated. The existence of a mixture of intermediates involving ring-cyclized and open-chain versions precluded the acquisition of a sharp carbon-13 spectrum, resulting in only a noisy spectrum which was illegible.

Effect of Bromide. Data in Figure 7a show that bromide ions catalyze the reaction by delivering shorter induction periods. There is a linear dependence between the inverse of the induction period and bromide concentrations when bromide concentrations are lower than the initial GTU concentrations. This catalytic effect levels off when added bromide concentrations approach and exceed GTU concentrations. Higher bromide concentrations not only reduce the induction period but also increase the rate and amount of final bromine concentrations produced. Figure 7b shows that there is a linear relationship between the maximum bromine concentrations obtained and the initial concentrations of bromide ions. This result is crucial in proving that there is no substantial bromination of the amino groups in guanylurea at the end of the reaction. The linear relationship confirms that the increase in bromine formed is based purely on the stoichiometry of reaction R2.

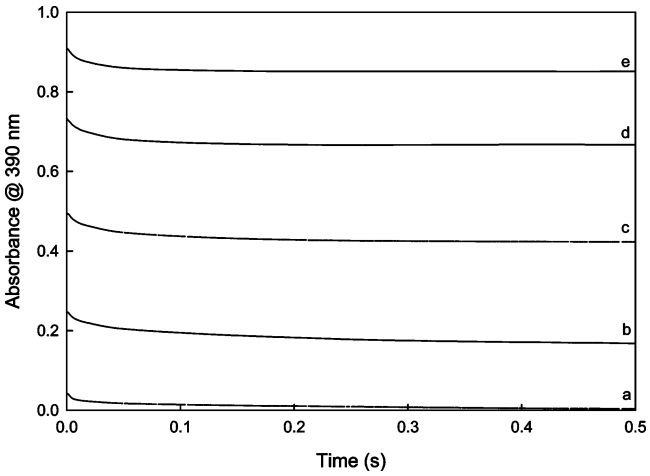

Figure 8. Absorbance traces for the rapid diffusion-controlled reaction between GTU and Br_2 showing the effect of progressively increasing bromine concentration. Simple absorbance calculations for all traces show that the stopped-flow technique cannot catch the consumption of the first 2 equiv of bromine for 1 equiv of GTU. $[GTU]_0 = 3 \times 10^{-4}$ M; $[Br_2]_0 =$ (a) 0.0015, (b) 0.003, (c) 0.0045, (d) 0.006, (e) 0.0075 M.

Reaction of Bromine and GTU. The direct reaction of aqueous bromine and GTU was extremely fast, approaching diffusion control, and was over in less than a second (see Figure 8). Utilizing the data in Figure 8 shows that the Hi-Tech Scientific stopped-flow ensemble could not capture the consumption of the first two equivalents of bromine. The stopped-flow ensemble could only catch the consumption of the third equivalent of bromine per one equivalent of GTU. The reaction was mildly inhibited by acid, but this inhibition was not sufficient to allow the monitoring of the consumption of the first two equivalents of bromine. We evaluated a lower limit bimolecular rate constant of $7.5 \pm 1.2 \times 10^4$ M^{-1} s^{-1} for the direct oxidation of GTU by aqueous bromine. This estimation was derived from data in Figure 8 where only the oxidation of the last two equivalents (stoichiometry R4) could be captured. The initial concentrations of bromine used for the calculation of the bimolecular rate constant were adjusted to account for this.

Reaction Mechanism

The standard oxybromine-based kinetics appears to dominate the initial stages of this reaction. The data in Figures 2b, 3b, and 7a suggest that the reaction is initiated by the formation of the reactive species $HBrO_2$ and HOBr:[23]

$$BrO_3^- + Br^- + 2H^+ \rightleftharpoons HBrO_2 + HOBr \qquad (R5)$$

The active oxidizing species in this mechanism would be HOBr, which, in a two-electron oxidation, would produce bromide which is recycled in reaction R5:

$$HOBr + 2e^- + H^+ \rightarrow Br^- + H_2O \qquad (R6)$$

The disproportionation of $HBrO_2$ is key to establishing the observed catalysis by bromide and the observed sigmoidal kinetics at 266 nm:

$$HBrO_2 + Br^- + H^+ \rightleftharpoons 2HOBr \qquad (R7)$$

Reaction R7 has been extensively studied and is considered to be extremely rapid.[24] In this case, the oxidation of the

SCHEME 1

Pathway A.

$H_2N(=NH)CNH(C=S)NH_2 \rightarrow H_2N(=NH)CN=(C\text{-}SOH)NH_2 \rightarrow$

(*sulfenic acid*)

$H_2N(=NH)CN=(C\text{-}SO_2H)NH_2 \rightarrow H_2N(=NH)CN=(C\text{-}SO_3H)NH_2 \rightarrow$

(*sulfinic acid*) (*sulfonic acid*)

$H_2N(=NH)CNH(C=O)NH_2 + SO_4^{2-}$ (not balanced)

(*guanylurea*)

Pathway B.

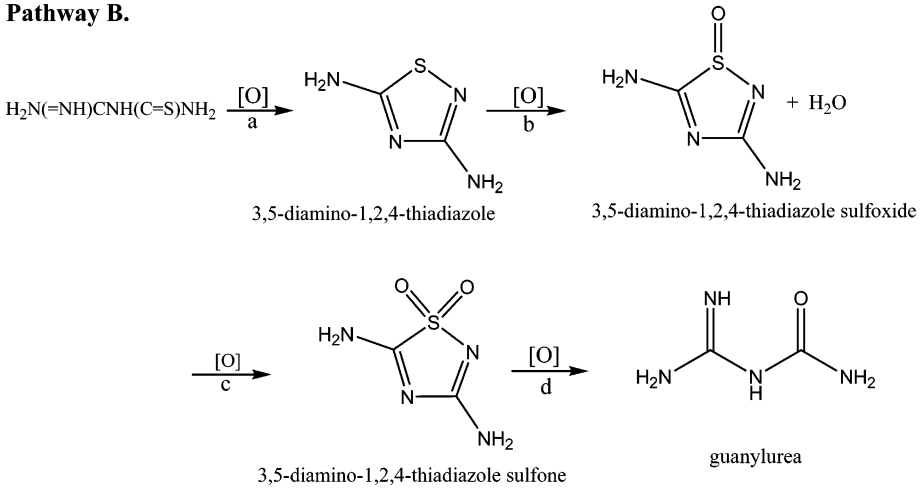

substrate by $HBrO_2$ can be considered negligible with the bulk of the oxidation proceeding through HOBr. However, at the beginning of the reaction, before accumulation of bromide occurs, the oxidation by bromous acid cannot be ignored. Addition of R5, 3R6, and R7 will show cubic autocatalysis in bromide ions:

$$BrO_3^- + 2Br^- + 6H^+ + 6e^- \rightarrow 3Br^- + 3H_2O \quad (R8)$$

Standard bromate concentrations contain approximately 10^{-6} M bromide ions which can initiate the oxidation of GTU through reaction R5. However, it will take much longer to build up effective concentrations of bromide and hence a sigmoidal, ever-increasing rate of reaction is observed. The catalytic effect of bromide saturates when initial bromide concentrations approach concentrations of the reducing substrate. At this point, the reaction kinetics will be dominated by reaction R5 from $t = 0$. This is also according to our experimental observations.

Oxidation of GTU. Previous studies on the oxidation mechanism of GTU by the mild oxidants iodine and acidic iodate had produced predominantly the cyclized version of a sulfenic acid.[14] Bromate oxidation proceeds to cleave the C−S bond to form sulfate and the urea analogue of GTU. There are two possible oxidation pathways (see Scheme 1). One would be the standard S-oxygenation pathway that generates the series of sulfur oxo-acids: sulfenic, sulfinic, and sulfonic acids followed by the formation of sulfate.[25] The other pathway would involve the initial oxidation to the five-membered 3,5-diamino-1,2,4-thiadiazole. Subsequent oxidations would involve the formation of the sulfoxide and the sulfone followed by the opening up of the ring to release sulfate and guanylurea.

Our inability to obtain a clean C-13 spectrum suggests a combination of both pathways, but data in Figure 5a,b suggest that the latter mechanism is dominant. For as long as reaction R5 is rate-determining, both pathways would be kinetically indistinguishable from each other. Rapid-scan techniques suggest that the unfolding of the cyclic sulfone (step d) into a linear chain sulfonic acid is responsible for the transient peak in absorbance at 266 nm observed near the end of the reaction. This peak was not significant at 390 nm, and thus computer simulations of the overall reaction scheme at 390 nm can be effected without considering the 266 nm transient peak.

Computer Simulations and Detailed Mechanism. In this study, reaction dynamics similar to those displayed in Figures 2a, 3a, 4a,b, and 7a were modeled based on a very simple mechanism that relied heavily on the well-known oxybromine kinetics.[24,26] The initial reaction was based on the formation of the sulfenic acid through oxygen atom transfer from hypobromous acid:

$$H_2N(=NH)CNH(C=S)NH_2 + HOBr \rightarrow H_2N(=NHCN=(C-SOH)NH_2 + Br^- + H^+ \quad (R9)$$

Formation of Br^- encourages further formation of HOBr through reaction R7. There is a very rapid reaction, the reverse of the disproportionation of bromine in aqueous solution which produces bromine:[27]

$$HOBr + Br^- + H^+ \rightleftharpoons Br_2 + H_2O \qquad k_{R10} = 8.9 \times 10^9\ M^{-2}\ s^{-1} \quad (R10)$$

Since the oxidation of GTU by aqueous bromine is very fast (see Figure 8), bromine will not accumulate until all the GTU and its subsequent oxo-acids are completely consumed (see Figure 5b).

$$H_2N(=NH)CNH(C=S)NH_2 + Br_2(aq) + H_2O \rightarrow H_2N(=NH)CN=(C-SOH)NH_2 + 2Br^- + 2H^+ \quad (R11)$$

It is irrelevant, for the modeling of the induction periods, if further oxidation goes through the ring-cyclized intermediates or through the standard oxo-acids. If one assumes the maintenance of the straight-chain analogues of the intermediates, we would assume continuous oxidation of the GTU by either HOBr or Br_2 all the way to sulfate.

$$H_2N(=NH)CN=(C-SOH)NH_2 + Br_2(aq) + H_2O \rightarrow H_2N(=NH)CN=(C-SO_2H)NH_2 + 2Br^- + 2H^+ \quad (R12)$$

$$H_2N(=NH)CN=(C-SO_2H)NH_2 + Br_2(aq) + H_2O \rightarrow H_2N(=NH)CN=(C-SO_3H)NH_2 + 2Br^- + 2H^+ \quad (R13)$$

The final step involves the simultaneous oxidation of the sulfur center to sulfate and the cleavage of the C−S bond.

$$H_2N(=NH)CN=(C-SO_3H)NH_2 + Br_2(aq) + 2H_2O \rightarrow H_2N(=NH)CNH(C=O)NH_2 + SO_4^{2-} + 4H^+ + 2Br^- \quad (R14)$$

Reactions R12−R14 can be rewritten with HOBr as the oxidant via an oxygen transfer mechanism.

Effect of Acid. The catalytic effect of acid on the whole reaction scheme is based on standard oxybromine kinetics. There was a slight retardation of the direct bromine−GTU reaction with acid, and this could come from two effects. The first effect could be as a result of the shift in the equilibrium of reaction R10[27] if HOBr oxidizes more rapidly than Br_2(aq), and the second effect could arise from the protonation of GTU[14] resulting in a protonated GTU species that reacts much more slowly with electrophilic groups such as Br_2(aq) and HOBr. There are a number of nucleophilic centers on the GTU molecule, but the most likely protonation centers are the thiol group and the distal carbon center to the thiol group: The

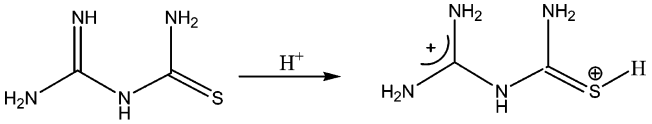

guanylthiourea (R15)

formation of the 3-center 4-electron site at the distal carbon deactivates the whole site from any electrophilic attack, and this includes the possible formation of N-bromamines as was observed with taurine.[28−30]

A rough calculation of the shift in equilibrium of reaction R10 shows very little difference in the [HOBr]/[Br_2] concentration ratios within the range of acid concentrations used in these studies. Hence the slight retardation observed with acid has its genesis from the protonation of the GTU. However, the reaction of the protonated GTU with either Br_2(aq) and with HOBr is still close to diffusion control and cannot be captured by our SF-DX2 stopped-flow spectrophotometer. The shortening of the induction period can only be attributed to the acid catalysis resident in reaction R5. R5 will be the rate-determining step all throughout the duration of the reaction after the buildup of enough bromide concentrations.

Reaction Initiation. The initial stages of the reaction involve the buildup of bromide concentrations. Our experimental data confirm that even though bromide ions are catalytic, this effect quickly saturates as the initial bromide concentrations added to the reaction mixture approach the concentrations of the substrate. There is a slow reaction between bromate and the substrate (R16 + R17) whose sole purpose is to build up bromide ions (apart from the 10^{-6} M that are present in standard bromate concentrations). The buildup of bromide ions activates reaction R5 which produces the oxidizing species HOBr and $HBrO_2$. The rapid protolytic equilibrium establishes bromic acid which then slowly reacts with GTU (written as $R(C=S)NH_2$ in this mechanism) to form bromous acid and the sulfenic acid:

$$BrO_3^- + H^+ \rightleftharpoons HBrO_3 \quad (R16)$$

$$HBrO_3 + R(C=S)NH_2 + H_2O \rightarrow HBrO_2 + R(CSOH)=NH \qquad k_{R17} \quad (R17)$$

The magnitute of k_{R17} was the single most important kinetics parameter in the simulations. It determined the induction period in Figures 3a and 4a,b. This value was adjusted for best fit, and a value of 44.2 M^{-1} s^{-1} was adopted. Further two-electron oxidation by $HBrO_2$ yields HOBr which will later react as in reaction R9 to produce bromide which is used in reaction R5.

$$HBrO_2 + R(C=S)NH_2 + H_2O \rightarrow HOBr + R(CSOH)=NH \quad (R18)$$

Since bromide ion production according to reaction R8 shows cubic autocatalysis, the buildup of bromide should be very rapid.

TABLE 1[a]

number	reaction	k_f; k_r
M1	$BrO_3^- + H^+ \rightleftharpoons HBrO_3$	1×10^7; 1×10^9
M2	$HBrO_3 + R(C=S)NH_2 \rightarrow HBrO_2 + R(CSOH)=NH$	44.2
M3	$HBrO_2 + R(C=S)NH_2 \rightarrow HOBr + R(CSOH)=NH$	5×10^2
M4	$HOBr + R(C=S)NH_2 \rightarrow R(CSOH)=NH + Br^- + H^+$	5×10^4
M5	$BrO_3^- + Br^- + 2H^+ \rightleftharpoons HBrO_2 + HOBr$	2.1; 1.0×10^4
M6	$HBrO_2 + Br^- + H^+ \rightleftharpoons 2HOBr$	2×10^9; 5×10^{-5}
M7	$HOBr + Br^- + H^+ \rightleftharpoons Br_2 + H_2O$	8.9×10^8; 110
M8	$Br_2 + R(C=S)NH_2 + H_2O \rightarrow R(CSOH)=NH + 2Br^- + 2H^+$	7.5×10^4
M9	$Br_2 + R(CSOH)=NH + H_2O \rightarrow R(CSO_2H)=NH + 2Br^- + 2H^+$	8×10^4
M10	$Br_2 + R(CSO_2H)=NH + H_2O \rightarrow R(CSO_3H)=NH + 2Br^- + 2H^+$	2.5×10^4
M11	$Br_2 + R(CSO_3H)=NH + H_2O \rightarrow R(C=O)NH_2 + SO_4^{2-} + 2Br^- + 4H^+$	1×10^3
M12	$HOBr + R(CSOH)=NH \rightarrow R(CSO_2H)=NH + Br^- + H^+$	6×10^4
M13	$HOBr + R(CSO_2H)=NH \rightarrow R(CSO_3H)=NH + Br^- + H^+$	1×10^4
M14	$HOBr + R(CSO_3H)=NH + H_2O \rightarrow R(C=O)NH_2 + SO_4^{2-} + Br^- + 2H^+$	1×10^3

[a] Legend: $R(C=S)NH_2$ = guanylthiourea; R(CSOH)=NH = guanylthiourea sulfenic acid; $R(CSO_2H)=NH$ = guanylthiourea sulfinic acid; $R(CSO_3H)=NH$ = guanylthiourea sulfonic acid; $R(C=O)NH_2$ = guanylurea. The sulfenic acid in this mechanism is equivalent to the ring-cyclized 3,5-diamino-1,2,4-thiadiazole, the sulfinic acid to the sulfoxide, and the sulfonic acid to the sulfone.

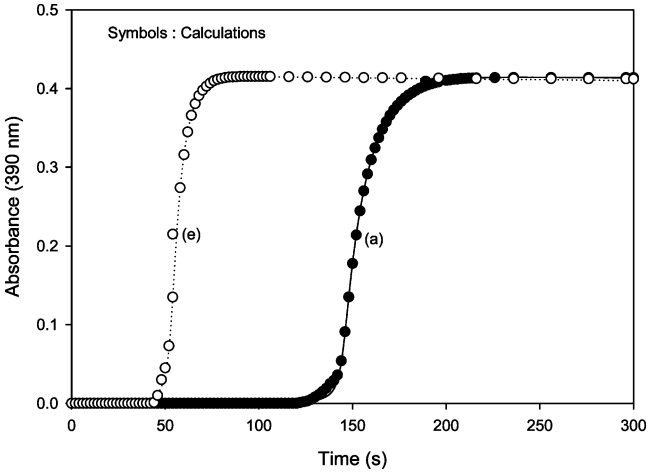

Figure 9. Computer modeling of the reaction for data shown in Figure 3a (traces a and e) using the scheme shown in Table 1. Symbols represent the calculated curves. There is satisfactory agreement between experiments and model.

Reactions R16 + R17 + R18 + R9 become irrelevant in conditions where bromide is initially added to the reaction mixture.

The final mechanism used for modeling the reaction scheme is shown in Table 1. By taking advantage of the rapid reaction R7, most of the reactions involving oxidations by $HBrO_2$ were ignored without adversely affecting the simulation results. For as long as all reactions involving the reduction of a bromine center coupled to the oxidation of a sulfur center were considered rapid and irreversible, the ultimate control of the reaction dynamics (rate, induction period, and bromine formation) was solely through oxyhalogen kinetics, and specifically reaction R5.

Explanation of Modeling Scheme and Source of Rate Constants. The software chosen for modeling this reaction scheme was the Kintecus model developed by James Ianni. To avoid termolecular reactions and above, solvent water was ignored throughout the simulations. Acid concentrations were taken as buffered without loss of precision. The software utilized, for example, could not handle the large number of products obtained in reactions M11 and M14, but this problem was then solved by keeping acid concentrations constant. Splitting reactions M11 and M14 also gave the same results, although the simulations were much slower after the addition of a rapid dissociation step that released the rest of the products in reactions M11 and M14. Reactions M11 and M14 were deliberately made slow for they represent the unfolding process to yield the straight-chain sulfonic acid analogue, followed by oxidation to yield sulfate and guanylurea.

The first four reactions in the scheme, M1−M4, were merely initiation reactions whose importance waned as the simulations proceeded. Their main contribution was the formation of bromide ions in reaction M4 (reactions of type R6 in the script) which gave way to autocatalytic production of bromide ions as in reaction R8. In the presence of added bromide ions, reactions M1−M4 could be removed with no visible changes observable in the results obtained from the model. The kinetics constants chosen for reaction M1 were not very important and could be varied widely for as long as they were (both) faster than any other reaction in the reaction medium (rapid protolytic reaction). The only limitation was the sluggishness of the simulations if high and realistic values of k_{M1} and k_{-M1} were used. The only use of reaction M1 was to allow for the setting up of reaction M2 as a bimolecular reaction rather than a termolecular one if reaction M1 was absent. Kinetics parameters for reactions M5−M7 were derived from established literature values.[20,26,31,32] The value of k_{M8} was derived from this study. After the determination of k_{M8}, subsequent kinetics parameters for reactions M9−M11 became ineffective in influencing the modeling results for as long as they were all faster or of the same magnitude as k_{M8}. The same idea was applied to the series of reactions M4, M12−M14. Thus the simulations were very simple, with k_{M2} being the only adjustable parameter, and in the presence of added bromide ions which shunted out reactions M1−M4, there were no adjustable rate constants. Figure 9 shows that the adopted model (Table 1) correctly predicts the data shown in Figure 3a. The model also satisfactorily predicted data in Figures 2a, 4a,b, 7a, and 8. It could also follow the initial parts of Figure 5a.

Acknowledgment. This work was supported by Research Grant Number CHE 0134375 from the National Science Foundation.

References and Notes

(1) Part 9 (of 10) in the series of publications to honor the memory of Dr. Cordelia R. Chinake, 3/18/65−11/2/98. Part 8: *J. Phys. Chem. A* **2004**, *108*, 1024−1032.
(2) Trochimczuk, A. W.; Kolarz, B. N. *Eur. Polym. J.* **2000**, *36*, 2359−2363.
(3) Kurien, M.; Kuriakose, A. P. *Plast., Rubber Compos.* **2001**, *30*, 263−269.
(4) Marykutty, C. V.; Mathew, G.; Mathew, E. J.; Thomas, S. *J. Appl. Polym. Sci.* **2003**, *90*, 3173−3182.
(5) Mini, V. T. E.; Mathew, C.; Kuriakose, A. P.; Francis, D. J. *J. Mater. Sci.* **1995**, *30*, 2049−2054.
(6) Susamma, A. P.; Kurian, M.; Kuriakose, A. P. *Iran. Polym. J.* **2002**, *11*, 311−323.
(7) Susamma, A. P.; Mini, V. T. E.; Kuriakose, A. P. *J. Appl. Polym. Sci.* **2001**, *79*, 1−8.
(8) Timofeev, N. N.; Frolov, S. F.; Zhitniuk, R. I. *Vestn. Khir. Im I. I. Grek.* **1975**, *115*, 39−43.
(9) Vertesi, C. *Med. Hypotheses* **1993**, *40*, 335−341.
(10) Gergely, P.; Lang, I.; Gonzalez-Cabello, R.; Feher, J. *Tokai J. Exp. Clin. Med.* **1986**, *11 Suppl*, 207−213.
(11) Busser, M. T.; Lutz, W. K. *Carcinogenesis* **1987**, *8*, 1433−1437.
(12) Jonnalagadda, S. B.; Chinake, C. R.; Simoyi, R. H. *J. Phys. Chem.* **1996**, *100*, 13521−13530.
(13) Darkwa, J.; Mundoma, C.; Simoyi, R. H. *J. Chem. Soc., Faraday Trans.* **1998**, *94*, 1971−1978.
(14) Chikwana, E.; Simoyi, R. H. *J. Phys. Chem. A* **2004**, *108*, 1024−1032.
(15) Makarov, S. V.; Mundoma, C.; Penn, J. H.; Svarovsky, S. A.; Simoyi, R. H. *J. Phys. Chem. A* **1998**, *102*, 6786−6792.
(16) Makarov, S. V.; Mundoma, C.; Svarovsky, S. A.; Shi, X.; Gannett, P. M.; Simoyi, R. H. *Arch. Biochem. Biophys.* **1999**, *367*, 289−296.
(17) Svarovsky, S. A.; Simoyi, R. H.; Makarov, S. V. *J. Phys. Chem. B* **2001**, *105*, 12634−12643.
(18) Svarovsky, S. A.; Simoyi, R. H.; Makarov, S. V. *J. Chem. Soc., Dalton Trans.* **2000**, 511−514.
(19) Chinake, C. R.; Simoyi, R. H. *J. Phys. Chem.* **1994**, *98*, 4012−4019.
(20) Lopez-Cueto, G.; Ostra, M.; Ubide, C. *Anal. Chim. Acta* **2001**, *445*, 117−126.
(21) Darkwa, J.; Olojo, R.; Olagunju, O.; Otoikhian, A.; Simoyi, R. *J. Phys. Chem. A* **2003**, *107*, 9834−9845.
(22) Jonnalagadda, S. B.; Chinake, C. R.; Simoyi, R. H. *J. Phys. Chem.* **1995**, *99*, 10231−10236.
(23) Chinake, C. R.; Simoyi, R. H.; Jonnalagadda, S. B. *J. Phys. Chem.* **1994**, *98*, 545−550.
(24) Noyes, R. M. *J. Am. Chem. Soc.* **1980**, *102*, 4644−4649.
(25) Chinake, C. R.; Simoyi, R. H. *J. Phys. Chem.* **1993**, *97*, 11569−11570.
(26) Noyes, R. M.; Field, R. J.; Thompson, R. C. *J. Am. Chem. Soc.* **1971**, *93*, 7315−7316.
(27) Kustin, K.; Eigen, M. *J. Am. Chem. Soc.* **1962**, *84*, 1355−1359.
(28) Chinake, C. R.; Simoyi, R. H. *J. Phys. Chem. B* **1998**, *102*, 10490−10497.
(29) Chinake, C. R.; Simoyi, R. H. *J. Phys. Chem. B* **1997**, *101*, 1207−1214.
(30) Simoyi, R. H.; Streete, K.; Mundoma, C.; Olojo, R. *South Afr. J. Chem.−Suid-Afrikaanse Tydskrif Vir Chemie* **2002**, *55*, 136−143.
(31) Sortes, C. E.; Faria, R. B. *J. Braz. Chem. Soc.* **2001**, *12*, 775−779.
(32) Szalai, I.; Oslonovitch, J.; Forsterling, H. D. *J. Phys. Chem. A* **2000**, *104*, 1495−1498.